Monthly Notices of the ROYAL ASTRONOMICAL SOCIETY
MNRAS **510,** 2167–2172 (2022) https://doi.org/10.1093/mnras/stab3636
Advance Access publication 2021 December 16

On the orbital velocity of isolated galaxy pairs: a test of gravity in the low acceleration regime

Riccardo Scarpa,[1,2]★ Renato Falomo[3] and Aldo Treves[4,5]

[1]Instituto de Astrofisica de Canarias, C/O Via Lactea, s/n, E-38205 La Laguna, Tenerife, Spain
[2]Departamento de Astrofsica, Universidad de La Laguna, E-38206 La Laguna, Tenerife, Spain
[3]INAF - Osservatorio Astronomico di Padova, vicolo dell'Osservatorio 5, I-35122 Padova, Italy
[4]Università dell'Insubria, via Valleggio 11, I-22100 Como, Italy
[5]INAF - Osservatorio Astronomico di Brera, via Bianchi 46, I-23807 Merate (Lecco), Italy

Accepted 2021 December 6. Received 2021 December 6; in original form 2021 September 30

ABSTRACT

The dynamics of isolated galaxy pairs represents an important tool to investigate the behaviour of gravity in the low acceleration regime. Statistical analysis of a large sample of galaxy pairs led to the noticeable discovery of a region of preferred 3-dimensional velocities centered at ∼150 and ∼100 km s^{-1} wide, a feature hard to justify in the context of numerical simulations of cosmological structure formation. It is shown here that such a feature is expected within the framework of the modified Newtonian dynamics, which, however, predicts it to be centered at ∼ 170 Km s^{-1}.

Key words: Gravitation – Galaxies: general – Galaxies: kinematics and dynamics – Dark matter.

1 INTRODUCTION

Many lines of investigations in present day astrophysics support the existence of large amounts of non-baryonic dark matter (DM hereafter) in galaxies and in the Universe at large. The most obvious example being the asymptotically flat rotation curve of galaxies, which posits for the existence of massive haloes of DM. Considerable fine tuning of DM content in galaxies is however required to justify their observed properties. The most striking example is possibly the baryonic Tully–Fisher relation (see e.g. McGaugh 2012, and reference therein). Because of this, over the years various proposals have been made to find alternative explanations, not involving DM. In particular, it has been shown that a specific modification of Newtonian dynamics (MOND, Milgrom 1983a,b,c) is able to describe many, if not all behaviours of galaxies generally ascribed to the presence of DM.

In search for new tests for both DM and alternative gravity theories, we focus here on isolated galaxy pairs as potential important probes of dynamics under gravity. In particular ,we examine in this paper the newly published Isolated Galactic Pair Catalog (IGPC, Nottale & Chamaraux 2018a, NC18a hereafter). We consider the detailed discussion presented in Nottale & Chamaraux (2020, NC20 hereafter), which starting from the available observable parameters – radial velocity difference, projected separation, and luminosity of the two components of each pair – were able to statistically recover the 3-dimensional orbital inter-velocity distribution. This led to the remarkable discovery of a preferred region for the orbital velocity (∼150 km s^{-1}). We discuss here the difficulties of explaining such a preferred orbital velocity within a conventional Newtonian framework, and consider alternative dynamical scenarios.

★ E-mail: riccardo.scarpa@gtc.iac.es

2 ISOLATED GALAXY PAIRS CATALOG

The IGPC was constructed by NC18a extracting the pairs from the HyperLEDA extragalactic data base (Makarov 2014). The following selection criteria were used: (1) absolute B magnitude of galaxies $M \leq -18.5$; (2) projected separation $r_p < 1$ Mpc; (3) radial velocity $3000 < v_r < 16\,000$ km s^{-1}; (4) radial velocity difference (intervelocity) $|\Delta V| < 500$ km s^{-1}; (5) exclusion of multiplets, each member is the closest to the other one; (6) isolation criterion $\rho = r_3/r_p$, where r_3 is the projected distance of the next nearest galaxy to the pair with $|\Delta V| < 500$ km s^{-1}. Taking $\rho \geq 2.5$ the catalog contains N = 13092 pairs satisfying the previous requirements, N = 7449 for $\rho \geq 5$, and N = 4599 for $\rho \geq 9$.

The analysis of the catalog is then reported in NC20, where the statistical methods, presented and validated in Nottale & Chamaraux (2018b, NC18b hereafter) for deprojecting an observed radial velocity distribution, are applied. The methods rest on the fact that the radial velocity component of a fixed 3D velocity v is uniformly distributed between 0 and v. NC20 applied the deprojection methods to several subsamples of their main catalog, finding in all cases the presence of a clear excess (a peak) of preferred intervelocities in the deprojected 3D distribution. The peak is centered at ∼150 km s^{-1} and has full width half maximum FWHM ∼100 km s^{-1}. This is shown in the upper panel of Fig. 1, which was reconstructed from the IGPC catalog following NC20 prescriptions (their fig. 4). Beside the peak at ∼150 km s^{-1}, the distribution of deprojected intervelocities is approximately constant in the 0 – 350 km s^{-1} range. Then, after a local minimum around 450 km s^{-1}, a second peak is present. This is not a real feature, rather, it is artificially produced by the deprojection technique, and represents the accumulation of those pairs with estimated 3D velocity larger than the 500 km s^{-1} limit imposed to the catalog. It is important to point out that the peak at ∼150 km s^{-1} is present, at the same location and width, in all subsamples irrespective of the value of

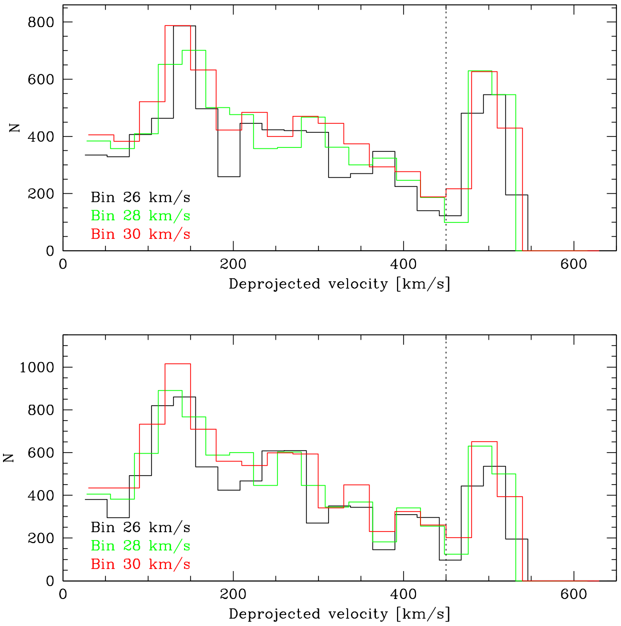

Figure 1. *Top panel:* de-projected 3D intervelocity of galaxy pairs from the isolated galaxy pairs catalog (as in NC20, their fig. 4), for the 7449 pairs with isolation parameter $\rho \geq 5$. Different bin sizes are used to show the position of the peak at $\sim$150 km s^{-1} is stable. *Bottom panel:* as for the top panel but considering 8571 pairs from our extended catalog. A very similar distribution is found. In both panels, instead of limiting the plot to 450 km s^{-1} (see dotted line) as in NC20, the full range of deprojected values is shown to highlight the presence of a large number of pairs at the end of the distribution. These are pairs with 3D intervelocity larger than the 500 km s^{-1} limit imposed to the catalog, most probably false unbound pairs.

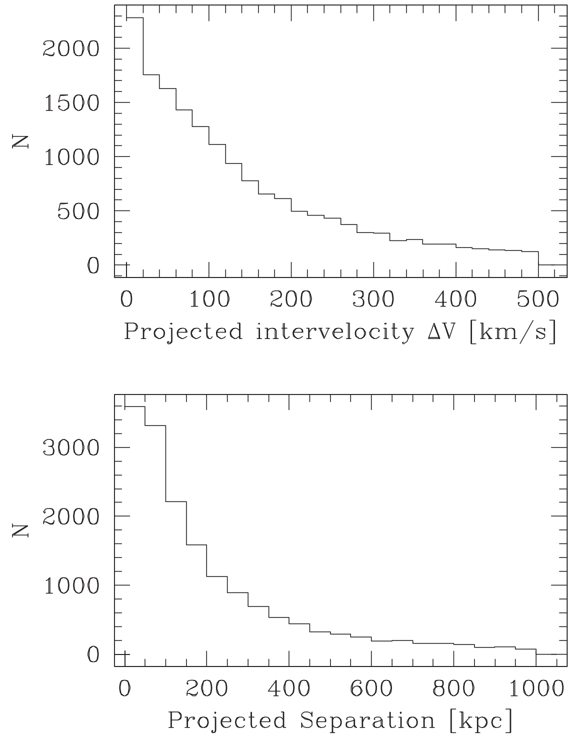

Figure 2. Distribution of projected intervelocity (upper panel) and projected separation (lower panel) for the 16 404 pairs in the extend catalog.

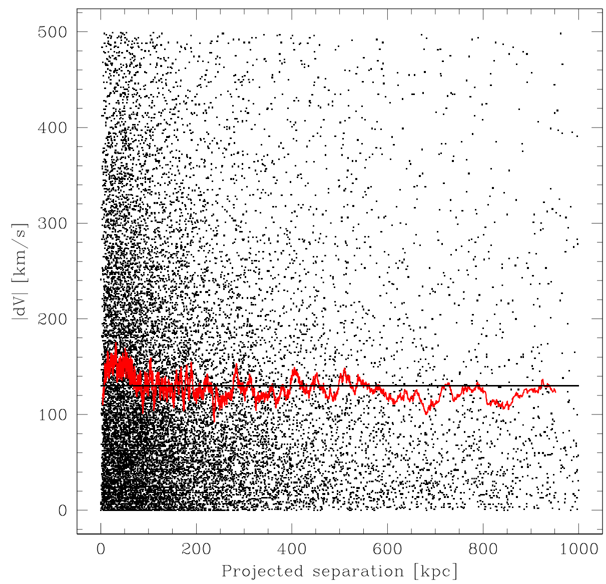

Figure 3. Observed intervelocities versus projected separation for the 16 404 galaxy pairs in the extended catalog. The red line gives the running average computed over 150 points, which is found to be sensibly constant over the whole range of projected separation. The horizontal line marks the global average of the sample.

ρ and/or filtering on radial velocity errors (see NC20 figs 3, 4, and 5).

Assuming most of the pairs are bound, NC20 showed that, on average, the virial mass of the pairs obtained through the 3D deprojection can be compared to their luminous mass provided the mass to light ratio is $M/L \sim 30$ (in solar units).

3 EXTENDED ISOLATED GALAXY PAIRS CATALOG

At the time of writing this paper, the Hyperleda catalog contained data for $\sim$ 5 millions galaxies, about 20 per cent more than at the time NC20 built their catalog. We focus here on this new larger sample of galaxies. There are $\sim$ 170 000 galaxies satisfying the selection criteria stated above (see Section 2). These were searched for pairs according to NC20 prescriptions, finding 16 404 pairs with $\rho \geq 2.5$, an increase of $\sim$25 per cent with respect to NC20 catalog. As expected and in line with NC20, most pairs are found at small projected separations and small velocity differences (see Figs 2 and 3).

The absolute magnitude of the selected galaxies is restricted to a range of about 3 magnitudes being limited by the galaxy luminosity function on the bright end, and by the cutoff at $M_B \leq -18.5$ at the faint end. The whole sample average luminosity is $M_B = 20.03$ with one σ dispersion of 0.87 mags (Fig. 4). The limited range of luminosity directly translates into a limited range of luminous masses, i.e. baryonic masses. Assuming M/L = 1 in solar units, masses spread a little more than an order of magnitude, with average total mass of the pairs 3.1×10^{10} M$_\odot$ (Fig. 5). No dependence of the mass on the projected distance is seen. Finally and particularly relevant for this work, applying the statistical method proposed by NC18b we derived the 3D deprojected intervelocity for this new extended catalog. The new distribution is

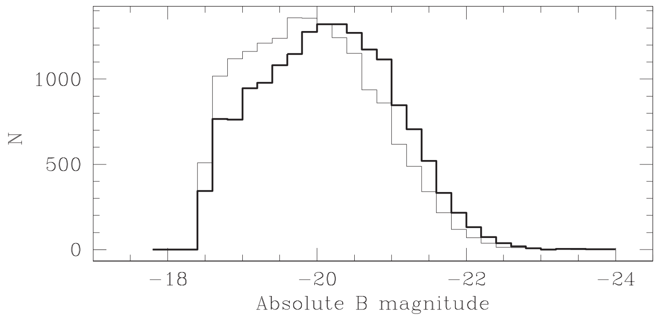

Figure 4. Distribution of B-band absolute magnitudes for all selected galaxies. Thick and thin histogram are for the primary and secondary component of the pairs.

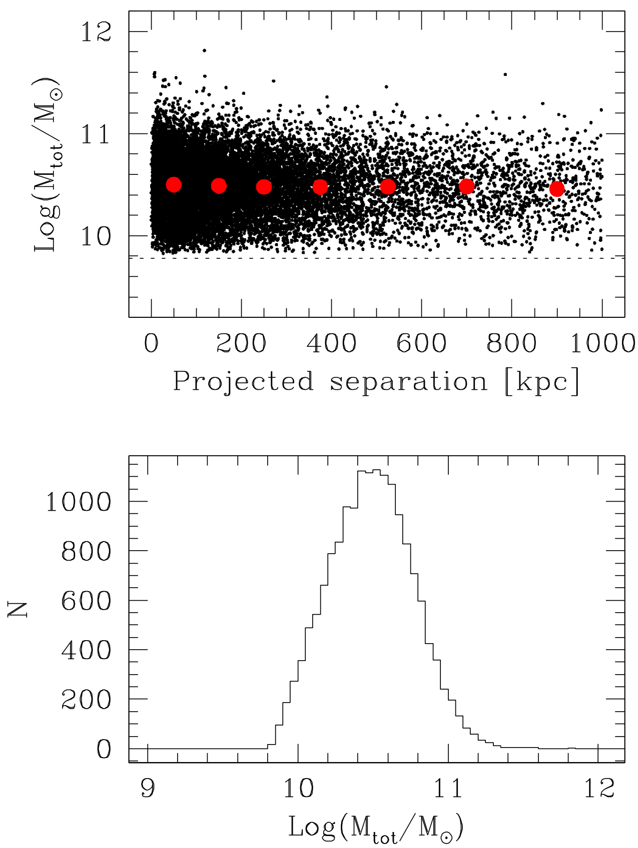

Figure 5. *Upper panel:* total luminous mass computed assuming M/L = 1 in solar units as a function of pair separation. Red points give the average mass in bins centered at increasing projected distance. The lower mass limit (dotted line) is due to the luminosity lower limit $M(B) < -18.5$ imposed to the catalog. *Lower panel:* distribution of the total luminous mass showing the limited range of masses covered by the catalog. The lack of objects at the lower end of the distribution is evident.

very similar to that derived by NC20 fully confirming the presence of a peak centered at ~ 150 km s^{-1} and including about 20 per cent of the pairs (Fig. 1, bottom panel). Tests with different bins and selection criteria confirm that the position and shape of the peak is stable.

To further estimate the statistical significance of the peak, we randomly selected half of the galaxies from the 8571 pairs as used to build fig. 1. Two bins before and after the peak were used to set the background level. The signal in the peak was defined as the sum of three bins (centered at 100, 130, and 160 km s^{-1}, see fig. 1) after subtracting the adjacent background. This was repeated 1000 times, finding the peak is present ~50 per cent of the times at $>5\sigma$ level, and ~90 per cent of the times at $>3\sigma$ level. Note that this significance represents a lower limit as it refers to half of the sample. Restricting the analysis to the 7499 pairs with accurate radial velocity ($\Delta V < 70$ km s^{-1}), the peak is even better defined being detected 60 per cent of the times at $>5\sigma$ and ~97 per cent of the times at $>3\sigma$ level.

4 FALSE PAIRS CONTAMINATION

A critical issue for the study of pair dynamics is to assess the level of unbound galaxy pairs present in the catalog, which was in fact built with no knowledge of whether individual pairs were bound systems or just chance alignments. In the catalog defined by NC20, it is assumed that most of the pairs form bound systems. However, if this were the case, the Newtonian velocity would represent a firm upper limit and therefore, on average, the projected ΔV should decrease with the pair separation as $r^{-1/2}$. No indication of such a behaviour is observed, the average ΔV remaining constant (Fig. 3). This suggests a significant fraction of pairs are unbound chance alignments.

A rough estimate of the level of contamination can be derived assuming the 170 000 galaxies from which our extended catalog was extracted, are uniformly distributed on the sky. The corresponding surface density is ~ 4 galaxies per square degree. At a representative radial velocity of 10 000 km s^{-1}, the adopted 1 Mpc maximum projected separation of pairs corresponds to ~ 0.5 square degrees ($H_0 = 70$ km s^{-1} Mpc^{-1} is used). Thus in each circle of radius 1 Mpc, we expect to find by chance ~ 2 galaxies. Then, because by construction the redshift is restricted to a range of 13 000 km s^{-1}, whatever the redshift of galaxy A, galaxy B has probability 1/13 to have redshift within ± 500 km s^{-1}. Dividing by two this probability to avoid counting pair AB and BA as two separate pairs, about 4 per cent or ~6800 pairs are expected by chance in our extended catalog, no matter if bound or not. Some of these candidate pairs will be eliminated by the requirement of not having other nearby galaxies within ± 500 km s^{-1}. This, however, has only a minor effect because a pair is retained on average in 12 out of 13 cases. Hence, the expected level of contamination is high (~ 40 per cent) and probably higher because the real data cover a significantly smaller fraction than the whole sky.

Another way to estimate the level of contamination is to count the number of pairs as a function of the *angular* separation (not projected separation), and compare it to the number of pairs found after a random permutation of their redshift (see Zhdanov & Surdej

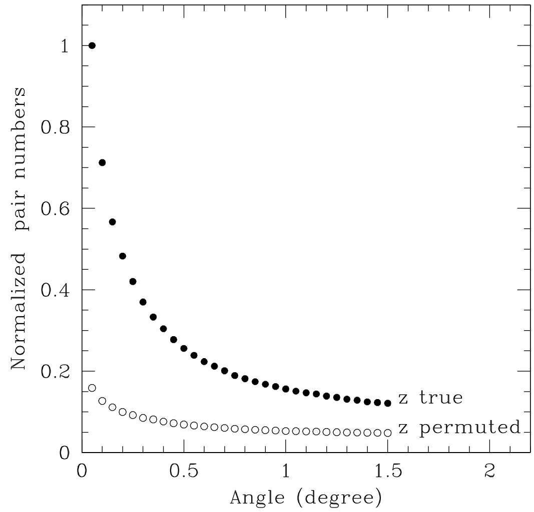

Figure 6. Comparison between the number of true galaxy pairs as a function of *angular* separation for the extended sample of ∼ 170 000 galaxies, and the same sample after random permutation of the radial velocity. The points are computed with a step of 0.05 degree and a redshift bin $\Delta V = 500$ km s^{-1}. The maximum angular separation shown (1.5 degree) corresponds to ∼ 1 Mpc at the lower limit of redshift in the sample.

2001 for more details). As expected ,the ratio between true and randomized galaxy pairs is higher at smaller separations (Fig. 6). In the explored range of angular separation (0.05 to 1.5 degree) there is about a total factor of 3.8 between the two data set, indicating at least 25 per cent of the galaxy pairs are just chance alignment of unbound pairs.

A further estimate of the amount of contamination was obtained searching for isolated pairs in a set of galaxies constructed using the same magnitudes and positions as for the true catalog, but with randomly permuted radial velocities. The full search was performed, including the limit in ΔV, the maximum projected separation, and the isolation criterion (see Section 2). In this shuffled data set ∼10 000 galaxy pairs were found, a value to be compared to the ∼16 000 pairs found in the real catalog. Thus ∼60 per cent of the pairs in the extended catalog could be unbound (just projected pairs).

All these tests indicate that a large fraction – possibly the majority – of pairs in NC20 and in our extended catalog are actually unbound pairs.

5 NEWTONIAN EXPECTATIONS FROM COSMOLOGICAL SIMULATIONS

In order to derive the expectations on the difference of velocity between the galaxies in pairs in the context of cosmological structure formation and evolution, we refer to the Millennium Simulation (Springel et al. 2005). In particular Moreno et al. (2013, hereinafter M13) used this Simulation to investigate the dynamical behaviour of galaxy pairs embedded in a full cosmological context. They extracted from the simulation a sample of about 1.3 million pairs having 3D separations smaller than 250h^{-1} kpc. This sample includes mainly pairs formed by either one central galaxy (inside a DM halo) and a satellite galaxy, or two satellite galaxies (in a larger DM halo). Based on these pair configurations, M13 derived the expected distribution of the true velocity difference of the galaxies in the pairs and found a very broad distribution ranging from few tens to about 2000 km s^{-1}.

No preferred orbital velocity was found by M13 in the Millenium simulation data. The distributions for the two types of pairs are shifted with respect to each other by about 400 km s^{-1}, and are both very wide having FWHM ∼800 km s^{-1}, in clear contrast with the sharp peak (FWHM ∼100 km s^{-1}) found in our analysis of IGPC. It is worth to note that our sample of pairs is different from that used by M13. First, following NC20, we defined galaxy pairs assuming a projected separation up to 1 Mpc compared to 250h^{-1} kpc adopted in M13. Then the median mass ratio of the pairs in our sample is ∼1.2, significantly smaller compared with that used by M13, that spreads over two orders of magnitude. Finally we note that while our galaxy pairs are unique and relatively isolated, those defined by M13 are not. The same galaxy in fact could be used to define more than one pair.

Due to all the above differences, it is arduous to compare the expected intervelocity of pairs formed in a full cosmological context to our sample. Nevertheless all M13 results clearly indicate that dynamical simulations do not predict a preferred intervelocity for galaxy pairs. A more specific simulation better matching our galaxy selection would be important to further reinforce (or weaken) the discrepancy.

6 AN ALTERNATIVE DYNAMICAL ANALYSIS

In view of the difficulties, within the expectation of Newtonian cosmological simulations, to explain the presence of a narrow peak in the intervelocity distribution of galaxy pairs, we explore here as an alternative the modified Newtonian dynamics (Milgrom 1983a,b,c). The basic idea of MOND is that Newtonian dynamics should be modified when the acceleration of gravity falls below a fixed value a_0. According to this proposal, the acceleration of gravity g is related to the Newtonian acceleration g_N by

$$g_N = g\mu(g/a_0). \tag{1}$$

The interpolation function $\mu(g/a_0)$, which is not defined by the theory, admits the asymptotic behaviour $\mu(g/a_0) = 1$ for $g >> a_0$, so to retrieve the Newtonian expression in the strong field regime, and $\mu(g/a_0) = g/a_0$ for $g << a_0$.

The value of a_0 must be derived observationally. Studying local galaxies Begeman, Broeils & Sanders (1991) found $a_0 \sim 1.2 \times 10^{-8}$ cm s^{-2}, which is the most widely adopted value. Later studies, however, proposed different values from as low as 0.9 (Bottema et al. 2002) to as high as 1.4 (see discussion in Gentile, Famaey & de Blok 2011).

Since the seminal papers by Milgrom (1983a,b,c), MOND has been applied to several astrophysical objects including (in order of increasing size) wide binary stars (Hernandez, Jiménez & Allen 2012; Hernandez, Cookson & Cortes 2021), Globular clusters (Scarpa, Marconi & Gilmozzi 2003; Scarpa & Falomo 2010; Scarpa et al. 2011; Hernandez & Lara-D I 2020), dwarf galaxies (Milgrom 1995; McGaugh & Milgrom 2013; Sanders 2021), gas dominated galaxies (McGaugh 2012; Sanders 2019), spiral galaxies (Sanders 1996; Gentile et al. 2011; Milgrom & Sanders 2007), elliptical galaxies (Milgrom & Sanders 2003; Durazo et al. 2018; Tian & Ko 2016), pair of galaxies (Milgrom 1983c), group of galaxies (Milgrom 2019; McGaugh et al. 2021), gravitational lenses (Sanders 2014), and cluster of galaxies (Sanders 1999, 2003). In all but one case, MOND succeeds in describing the observations without the need of DM. The only case in which an excess of mass (by a factor two) is found between observations and MOND prediction is in rich clusters of galaxies. This is a long standing, unsolved problem for MOND that, however, does not falsify the theory because it points to the existence of still to be discovered baryonic mass in clusters. For

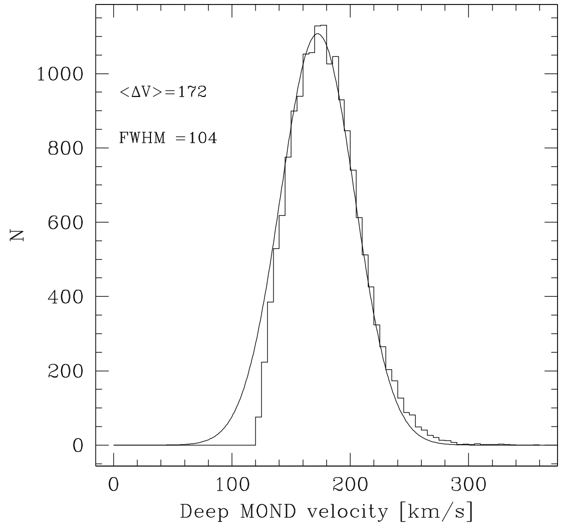

Figure 7. Predicted deep MOND intervelocity distribution, computed according to equation 3 and assuming a mass to light ratio M/L = 1 (in solar units). Data are well described by a Gaussian (with average and full width at half maximum as indicated). The mismatch at the lower velocities being due to the missing low mass pairs.

further reading and recent reviews see Famaey & McGaugh (2012), and Merritt (2020).

Assuming there are only baryons, the mass distribution in galaxies is such that the MOND regime is reached for distances smaller or comparable to the size of the galaxies themselves. Thus, when considering the dynamics of galaxy pairs, even the closest ones, the exact shape of the interpolation function μ is irrelevant. Everything takes place in deep MOND regime where the acceleration becomes

$$g = \sqrt{g_N a_0}. \qquad (2)$$

At present, no fully fledged numerical simulations developed within the framework of MOND exist. Therefore, only a crude approximation can be made of what galaxy pair dynamics should be. Here, we consider the approximate formula eq. 3 proposed by Milgrom (1983c) giving the expected velocity difference ΔV for galaxy pairs in the simple case of circular motion and equal mass M of the two components:

$$\Delta V^4 = 2GM_{tot}a_0, \qquad (3)$$

where $M_{tot} = 2M$ is the total mass of the pair. A more detailed analysis including the formalism presented in Milgrom (1994) will be presented in a future work. Note the lack of dependence of ΔV on the pair separation. This is a key characteristic of MOND which recovers the Tully–Fisher relation (Tully & Fisher 1977).

In order to reconstruct the distribution of the orbital velocity under the MOND framework, one should start from the luminous mass distribution (Fig. 5) using the formula (3). The resulting intervelocity distribution is well matched by a Gaussian with average $<V>$ =172 km s^{-1} and FWHM =104 km s^{-1} (Fig. 7). The lack of dependence of the velocity on separation, and the $M^{1/4}$ dependence of the velocity in MOND, further combined with the luminosity limits applied to the catalog, has the effect that only a very limited range of orbital velocities for galaxy pairs is permitted. Neither too small nor too large velocities are allowed. The MOND distribution clearly suggest the existence of a region of preferred velocity, which directly compare to the peak at $\sim$ 150 km s^{-1} observed in the 3D deprojection of the intervelocity (Fig. 1). Both peaks have similar width, though are shifted by about $\sim$ 20 km s^{-1}. In this framework therefore the pairs outside the peak represents unbound systems.

7 DISCUSSION AND CONCLUSIONS

We analysed the properties of the 3D intervelocity distribution of a sample of isolated galaxy pairs. The sample is an important laboratory for studying galaxy pair dynamics and led to the remarkable discovery of a preferred 3D intervelocity of $\sim$150 km s^{-1} (NC20). Within the framework of Newtonian dynamics, there is no straightforward explanation for the existence of a preferred orbital velocity, a point already recognized by NC20. While an explanation in the Newtonian dynamics with some *ad hoc* hypothesis (e.g. an adequate DM distribution) cannot be excluded, it is of interest to explore alternative interpretations. In particular, for this sample of galaxy pairs MOND predicts the existence of a narrow distribution of orbital velocities –as wide as the observed one – centered at 170 Km s^{-1}. The limited range of orbital velocities is due to the pairs being in deep MOND regime, so that the pair separation becomes irrelevant in determining the orbital velocity. The observed peak accounts for $\sim$20 per cent of the total galaxy pairs. In this scenario the remaining pairs represent unbound systems as discussed in Section 4.

Note that the peak expected in the MOND interpretation is at $\sim$ 170 km s^{-1} while that derived from the deprojection analysis is at $\sim$ 150 km s^{-1}. Taking at face value this 20 km s^{-1} difference, to match the observations to the prediction from equation 3 – which is itself approximate (Milgrom 1983c) – a reduction of a factor $\sim$2 is required on the right-hand side of equation 3. Among the many possible sources for this mismatch we mention: (i) a_0 could be smaller than the generally adopted value, (ii) the bound pairs might have on average lower luminosity than the unbound pairs, (iii) the mass to light ratio for bound systems could be significantly different than the value adopted here. For instance, taking $a_0 = 0.9 \times 10^{-8}$, a value at the lower end of the one reported in the literature (Bottema et al. 2002), the mismatch is halved (peak center at 160 km s^{-1}). Further computing luminous masses adopting $H_0 = 74$ km s^{-1} Mpc^{-1} which is more appropriate for the local Universe (Riess et al. 2019), instead of 70 km s^{-1} Mpc^{-1} as used in Hyperleda, would additionally move the peak velocity to 155 km s^{-1}. On the other hand, if the mass to light ratio were significantly higher than M/L = 1 adopted here the mismatch would be larger. For M/L = 2 the peak velocity would move to $\sim$ 200 km s^{-1}, a value uncomfortably large for the MOND interpretation.

It is clear, however, that the relevant aspect of this investigation is not the exact position of the peak, which depends on a number of parameters and the adopted modification of Newtonian gravity. Rather, it is that the velocity distribution of isolated galaxy pairs may be relevant for constraining the dynamics in the low acceleration regime, and in this contest alternative dynamical scenarios, like MOND, should be taken in serious consideration.

ACKNOWLEDGEMENTS

We are grateful to the anonymous referee for useful comments and suggestions.

DATA AVAILABILITY

The data supporting the findings of this study are openly available at Hyperleda web site (http://leda.univ-lyon1.fr).

REFERENCES

Begeman K. G., Broeils A. H., Sanders R. H., 1991, MNRAS, 249, 523
Bottema R., Pestaña J. L. G., Rothberg B., Sanders R. H., 2002, A&A, 393, 453
Durazo R., Hernandez X., Cervantes Sodi B., Sanchez S. F., 2018, ApJ, 863, 107
Famaey B., McGaugh S. S., 2012, LRR, 15, 10
Gentile G., Famaey B., de Blok W. J. G., 2011, A&A, 527, 76
Hernandez X., Cookson S., Cortes R. A. M., 2021, MNRAS, preprint (arXiv:2107.14797)
Hernandez X., Jiménez M. A., Allen C., 2012, Eur. Phys. J., 72, 1884
Hernandez X., Lara-D I A. J., 2020, MNRAS, 491, 272
Makarov D., Prugniel P., Terekhova N., Courtois H., Vauglin I., 2014, A&A, 570, 13
McGaugh S. S., 2012, AJ, 143, 40
McGaugh S. S., Lelli F., Schombert J. M., Li P., Visgaitis T., Parker K.S., Pawlowski M.S., 2021, AJ, 162, 202
McGaugh S. S., Milgrom M., 2013, ApJ, 766, 22
Merritt D., 2020, A philosophical approach to MOND. Cambridge Univ. Press, Cambridge
Milgrom M., Sanders R. H., 2007, ApjL, 658, 17
Milgrom M., 1983a, ApJ, 270, 365
Milgrom M., 1983b, ApJ, 270, 371
Milgrom M., 1983c, ApJ, 270, 384
Milgrom M., 1994, ApJ, 429, 540
Milgrom M., 1995, ApJ, 455, 439
Milgrom M., 2019, Phys. Rev. D, 99, 4041
Milgrom M., Sanders R. H., 2003, ApJ, 599, 25
Moreno J. et al., 2013, MNRAS, 436, 1765
Nottale L., Chamaraux P., 2018a, Astrophys. Bull., 73, 310
Nottale L., Chamaraux P., 2018b, A&A, 614, 45
Nottale L., Chamaraux P., 2020, A&A, 641, 115
Riess A. G., Casertano S., Yuan W., Macri L.M., Scolnic D., 2019, ApJ, 876, 85
Sanders R. H., 1996, ApJ, 473, 117
Sanders R. H., 1999, ApJ, 512, 23
Sanders R. H., 2003, MNRAS, 342, 901
Sanders R. H., 2014, MNRAS, 439, 1781
Sanders R. H., 2019, MNRAS, 485, 513
Sanders R. H., 2021, MNRAS, 507, 803
Scarpa R., Falomo R., 2010, A&A, 523, 43
Scarpa R., Marconi G., Carraro G., Falomo R., Villanova S., 2011, A&A, 525, 148
Scarpa R., Marconi G., Gilmozzi R., 2003, A&AL, 405, 15
Springel V. et al., 2005, Nature, 435, 629
Tian Y., Ko C., 2016, MNRAS, 462, 1092
Tully R. B., Fisher J. R., 1977, A&A, 54, 661
Zhdanov V. I., Surdej J., 2001, A&A, 372, 1

This paper has been typeset from a TEX/LATEX file prepared by the author.